

## ARTICLES

 **${}^2\text{H}(p, 2p)n$  reaction at 508 MeV: Recoil momentum  $> 200$  MeV/c**

M. B. Epstein,<sup>(1)</sup> J. P. Huber,<sup>(1)</sup> K. A. Aniol,<sup>(1)</sup> A. Bracco,<sup>(2)\*</sup> C. A. Davis,<sup>(2)†</sup> H. P. Gubler,<sup>(2)‡</sup>  
 W. P. Lee,<sup>(2)§</sup> D. J. Margaziotis,<sup>(1)</sup> C. F. Perdrisat,<sup>(3)</sup> P. R. Poffenberger,<sup>(2)\*\*</sup> H. Postma,<sup>(4)</sup>  
 V. Punjabi,<sup>(3)††</sup> H. J. Sebel,<sup>(4)‡‡</sup> A. W. Stetz,<sup>(5)</sup> and W. T. H. van Oers<sup>(2)</sup>

<sup>(1)</sup>California State University, Los Angeles, Los Angeles, California 90032

<sup>(2)</sup>University of Manitoba, Winnipeg, Manitoba, Canada R3T 2N2

<sup>(3)</sup>College of William and Mary, Williamsburg, Virginia 23185

<sup>(4)</sup>University of Technology, Delft, The Netherlands

<sup>(5)</sup>Oregon State University, Corvallis, Oregon 97331

(Received 5 April 1990)

Differential cross sections are presented for the reaction  ${}^2\text{H}(p, 2p)n$  at  $T_p = 507$  and 508 MeV for neutron recoil momenta ranging from 200 to 670 MeV/c. Data were taken for a wide range of kinematic conditions in which the relative kinetic energy between pairs of particles in the final state varied from 12 to 318 MeV. The data are compared with the impulse approximation (IA), which includes both  $p$ - $p$  and  $p$ - $n$  knockout terms, as well as with a nonrelativistic Glauber theory calculation (MS), which describes double scattering and final state interactions. The MS calculation agrees well with most of the data and is a significant improvement over the IA. Some of the data show evidence of virtual  $\Delta$  excitation in the final state.

## I. INTRODUCTION

This is the second part of our recent study of the  ${}^2\text{H}(p, 2n)n$  reaction at 508 MeV. Part I<sup>(1)</sup> has dealt largely with the data for which the unobserved neutron has recoil momentum,  $p_5$ , of 0 to 200 MeV/c. This paper will discuss the data for  $p_5$  of 200 to 670 MeV/c. (Some of these data have been previously published.<sup>2</sup>) Since Ref. 1 describes much of the relevant background information and details of the experimental procedure and equipment we will only provide a brief summary of this information here. A more detailed discussion will be given for those aspects of this part of our measurement which differ significantly from what has been described in part I.

The single nucleon knockout reactions  ${}^2\text{H}(p, 2p)n$  and  ${}^2\text{H}(e, e'p)n$  are the simplest possible reactions of this type that one can study and as such may provide the best place in which to compare detailed calculations with data. The momenta of interest are defined as follows:  $\mathbf{p}_1$ =incident beam,  $\mathbf{p}_2$ =target,  $\mathbf{p}_3$ =scattered proton,  $\mathbf{p}_4$ =ejected proton,  $\mathbf{p}_5$ =spectator neutron. In the impulse approximation (IA), for proton knockout, the reaction proceeds by the interaction of the incident proton with the target proton. The neutron is left unaffected and its final-state recoil momentum is assumed to be the same as the momentum it had initially in the target deuteron. The cross section can thus be written as

$$\frac{d^3\sigma}{d\Omega_3 d\Omega_4 dT_3} = K \left| \frac{d\sigma}{d\Omega} \right| |\Phi(\mathbf{p}_5)|^2, \quad (1)$$

where  $k$  is a kinematic factor,  $d\sigma/d\Omega$  is the half-off-shell proton-proton elastic scattering differential cross section, and  $|\Phi(\mathbf{p}_5)|^2$  is the single nucleon momentum density which is equal to the spectral function,  $S(\mathbf{p}_5, E)$  with  $E$  equal to the binding energy of the deuteron. Knockout reactions of this type have been used<sup>3,4</sup> to measure the spectral function  $S(\mathbf{p}_5, E)$  for many nuclei. These studies have met with mixed success. One would hope that a careful study of the  ${}^2\text{H}(p, 2p)n$  and  ${}^2\text{H}(e, e'p)n$  reactions would provide important insights as to the validity of this approach to obtaining information on  $S(\mathbf{p}_5, E)$  in general as well as giving useful information on the nature of the important reaction mechanisms involved.

Part I of this work concentrated on obtaining high precision data in a region where the impulse approximation is dominant. From these studies one gets a measure of the spectral strength of the proton in the deuteron. The data presented here probe a more complex region in which the impulse approximation is no longer the overwhelmingly dominant mechanism and more complex features of the deuteron wave function such as the  $D$  state and short-range components become quite important.

The  ${}^2\text{H}(e, e'p)n$  reaction<sup>5,6</sup> has recently been measured up to  $p_5$  of 500 MeV. The data are in fairly good agreement with calculations done by Arenhövel<sup>7</sup> in which meson exchange and final-state interactions are explicitly taken into account. One notes that these nonimpulse approximation terms are quite important here. Existing  ${}^2\text{H}(p, 2p)n$  data<sup>8</sup> cover the region  $0 < p_5 < 400$  MeV/c, and are not well understood. The data above  $p_5 > 200$  MeV/c are larger than the IA by as much as a factor of

10. So far no consistent and satisfactory interpretation has been available for these large recoil data. A multiple scattering calculation done by Wallace<sup>9</sup> specifically for the symmetric angular correlation data of Perdrisat *et al.*<sup>8</sup> failed to reproduce these data by a factor of 8. As a consequence of this systematic disagreement with the IA, single particle momentum wave functions calculated from the data with formula (1) for a given recoil momentum, but for different kinematics, have given different results, casting doubt about the simple physical interpretation of  $(p,2p)$  data. Very recently data taken at an incident proton energy of 1 GeV (Ref. 10) have been presented for  $0 < p_5 < 290$  MeV/c. These data appear to agree fairly well with both the PWIA and multiple scattering calculations. We note that these data were normalized to their calculation at the lowest values of  $p_5$  and are therefore not precise absolute cross-section measurements.

Our objective is to provide an experimentally consistent set of data for  $200 < p_5 < 670$  MeV/c that cover a wide range of the final-state two-body relative energies  $T_{34}$ ,  $T_{45}$ , and  $T_{35}$ . ( $T_{ij}$  is the kinetic energy of nucleons  $i$  and  $j$  in the two-nucleon center of mass system.) The smallest relative energy occurring in the present data is 12 MeV, which is too large to see the FSI enhancement observed by Witten *et al.*<sup>8</sup> Most of the existing data have at least one of the  $T_{ij}$  values close to 300 MeV, a situation which has been presumed to favor virtual  $\Delta$  excitation in the  $ij$  pair. We have obtained data in kinematics with all three  $T_{ij}$ 's as far away from 300 MeV as possible to minimize the effect of the  $\Delta$  excitation, as well as in the  $\Delta$  excitation region to maximize it. These data are compared with a calculation based on the work of Wallace<sup>9</sup> and we find substantial agreement between this calculation and the data; agreement which is much better than had been achieved in the past. Ultimately a comparison of these data with the  ${}^2\text{H}(e,e'p)n$  data should provide a more reliable description of the large single nucleon momentum region of the deuteron system.

## II. EXPERIMENTAL METHOD

The experiment was done at the TRIUMF cyclotron laboratory over a period of two years. The data were taken using the magnetic spectrometer (MRS) on the left-hand side of the beam and an array of counter telescopes on the right-hand side. These counter telescopes consisted of a thin plastic scintillator followed by a NaI(Tl) detector. When needed a copper absorber was placed in front of the NaI(Tl) detector to provide sufficient material to stop the protons of interest. In the first part, done in 1983 (Expt 83) the proton beam energy was  $507 \pm 1$  MeV and data were taken for the angle pairs  $\theta_3$ - $\theta_4$ :  $66.0^\circ$ - $66.0^\circ$ ,  $57.0^\circ$ - $57.0^\circ$ ,  $52.0^\circ$ - $52.0^\circ$ ,  $52.0^\circ$ - $66.0^\circ$ ,  $57.0^\circ$ - $66.0^\circ$ , and  $66.0^\circ$ - $53.6^\circ$ . In the second part done in 1984 (Expt 84) the beam energy was  $508 \pm 1$  MeV. Data were taken with the MRS at  $30.0^\circ$  and the counter telescopes at  $68.0^\circ$ ,  $75.0^\circ$ ,  $83.0^\circ$ , and  $90.0^\circ$ . In addition, data were taken for the angle pairs  $41.5^\circ$ - $57.0^\circ$ ,  $41.5^\circ$ - $68.0^\circ$ , as well as with the MRS at  $14.0^\circ$  and the counter telescopes at  $53.75^\circ$ ,  $62.0^\circ$ ,  $73.0^\circ$ , and  $85.0^\circ$ . The  $14.0^\circ$  data generally define kinematics that

are far from the region of  $\Delta$  excitation. The  $30.0^\circ$  data and some of the other data are very close to or right on the  $\Delta$  resonance. For all the data the solid angles on the right-hand side were defined by the plastic scintillators. These scintillators were typically 6.35 cm in diameter and were placed 200 cm from the center of the target. For Expt 83 the MRS solid angle was defined by software cuts on the front end multiwire proportional counter. For Expt 84 the MRS solid angle was defined by a 3.5-cm diameter circular plastic scintillator ( $\Delta E_{b1}$ ) placed in front of it. This scintillator was at 135.0 cm from the center of the target. Hardware triggers were formed by a fast timing coincidence between front end plastic scintillators on the left- and right-hand sides along with a timing signal that determined that a charged particle had arrived at the focal plane of the MRS. For Expt 84 the MRS focal plane instrumentation consisted of two vertical drift chambers (VDC) placed about the focal plane and an array of ten plastic scintillators placed behind the last VDC. For Expt 83 multiwire proportional counters and two large plastic scintillators were used to read out the focal plane information. A liquid deuterium target was used. The target thickness was approximately 0.8 cm. The precise thickness was determined by filling the target cell with liquid hydrogen, measuring  $p$ - $p$  elastic scattering, and comparing the results with precision data already in existence.

## III. DATA ANALYSIS

The symmetric angle data from Expt 83 were analyzed at the College of William and Mary in the manner described in Ref. 1 with the addition of software cuts on the energy of the protons detected in the NaI(Tl) counter telescopes. These additional cuts were needed only for the high  $p_5$  data in order to eliminate events in which the total energy of the unobserved particle was not equal to the mass of a neutron. The data from Expt 84 and the asymmetric angle data from Expt 83 were analyzed event by event at California State University, Los Angeles, using programs written for the Unix operating system on a Ridge-32 minicomputer. The analysis was similar to that done for the Expt 83 data but differed in part due to the differences in the experimental setup between Expt 83 and Expt 84.

For Expt 84 the data were first subjected to a series of tests which restricted them to those events that satisfied the timing requirements for real events in which the time of flight of the particle detected in the MRS was consistent with it being a proton. Cuts were then placed on the pulse heights of all the plastic scintillators and the NaI(Tl) detectors to eliminate noise and signals due to low ionizing particles. For the MRS the VDC that was behind the focal plane had several dead wires which effectively cut out a significant part of the focal plane. By analyzing data using only the front VDC in the region unaffected by these wires and analyzing the same data using both VDC's we determined that it was possible to use only the front VDC without any significant loss of momentum resolution. Events were characterized as good in the front VDC if only one cluster of wires were

hit, if there were no gaps between wires in this cluster and if no less than three and no more than seven wires were hit. The efficiency of the VDC was measured by restricting the data to a subset of events which satisfied the time-of-flight requirement for protons in the MRS and did not hit the plastic scintillators that were on the extreme edges in the dispersion direction of the focal plane. The efficiency was then taken as the number of events in this subset which were also characterized as good in the VDC divided by the total number of events in this subset. The pulse height information from the NaI(Tl) and the MRS detectors was converted to momenta after being corrected for energy losses in absorbing materials in front of them, and then combined to form missing energy spectra for the unobserved neutrons. Software cuts were placed on these spectra to restrict analysis to those events which had a missing mass equal to that of a neutron. In this manner we eliminated events for which a real pion can exist in the final state and greatly reduced the number of accidental coincidences due to low energy protons.

As described in Ref. 1 measurement of the electronic and computer live time was done by counting the number of pulses stored and the number of pulses sent from a pulser which drove light emitting diodes (LED) which were mounted in the light pipes of all the plastic scintillators and NaI(Tl) crystals. Accidental coincidences were distinguished from real coincidences by putting software cuts on the coincidence time spectrum. Accidentals were analyzed in exactly the same manner as real events and were subtracted from real coincidences. Pulse pile up in the NaI(Tl) crystals was measured by calculating the ratio of LED pulser signals in the main, narrow peak in the NaI(Tl) pulser pulse height spectrum to the total number of LED pulser signals in this spectrum. The pile up correction was usually only of the order of a few percent.

The data were then binned as a function of  $T_3$ , the kinetic energy of the protons detected in the MRS. The width of this bin varied from 5 to 10 MeV for the different angle pairs. The resulting data were corrected for computer dead time, VDC efficiency, and pile up losses discussed above as well as for reaction losses in the NaI(Tl) and copper in the right-hand side counters.<sup>11</sup> The corrected data were then converted to threefold differential cross sections  $d^3\sigma/d\Omega_3d\Omega_4dT_3$ .

#### IV. RESOLUTION AND ERROR ANALYSIS

As discussed in Ref. 1 the angular acceptances of the detectors along with the energy bin for  $T_3$  introduced a width for the measured momenta  $\mathbf{p}_3$  and  $\mathbf{p}_4$  as well as for the calculated momentum  $\mathbf{p}_5$ . In addition if one weighs the acceptances by the PWIA predictions there is a slight shift in the average value of  $p_5$  away from the kinematic central value. For these data this shift is only 2 to 3 MeV/c and will be ignored here. The full width at half maximum of the inferred acceptance for  $p_5$  varied from about 20 MeV/c to 40 MeV/c with most of the data having a width closer to 20 MeV/c.

Systematic errors include uncertainties in the target density, the solid angles, the beam current normalization, and estimates of the various efficiencies. Since we were

able to normalize our data to high precision  $p$ - $p$  differential cross-section data<sup>1</sup> these systematic errors are fairly small and are estimated for Expt 84 to be  $\pm 5\%$ . For Expt 83 the systematic errors are a bit larger and are estimated to be  $\pm 7\%$ . In the presentation of the data in the following sections this systematic error is not included and in all but one case only statistical errors are shown.

For the angular pair  $\theta_3=30^\circ$ ,  $\theta_4=83^\circ$  there is an additional source of error due to the fact that these angles were also the correct angles for  $p$ - $d$  elastic scattering in which the deuterons are at  $30^\circ$  in the MRS and protons are at  $83^\circ$  in the NaI(Tl) counter. The momentum bite in the MRS was not set for these elastic scattered deuterons but, through multiple scattering, some managed to get to the focal plane and provided a fairly large background underneath the relatively small  ${}^2\text{H}(p,2p)n$  data of interest. It was not possible to identify cleanly these particles as deuterons without some additional losses in efficiency in the MRS and consequently some additional errors for some of the data for these angles. These errors are included in the data shown in the following sections.

#### V. IMPULSE APPROXIMATION AND MULTIPLE SCATTERING CALCULATIONS

Since the data shown in the next section will be compared to both IA and multiple scattering calculations these calculations will be described in this section first. For  $p_5 > 300$  MeV/c it becomes necessary, in the context of the IA, to include neutron as well as proton knockout. That is, one must consider that the observed proton with momentum  $\mathbf{p}_4$  is the spectator particle and the unobserved neutron was the particle directly knocked out by the incident proton. The reason for including this process is that as  $p_5$  increases  $p_4$  tends to decrease and one reaches a point where  $|\Phi(\mathbf{p}_4)|^2$  becomes comparable in magnitude to  $|\Phi(\mathbf{p}_5)|^2$ . Thus, as can be seen from Eq. (1), the amplitudes of these two processes become more nearly equal. The IA calculation used here therefore includes the coherent addition of both terms. In addition to these two IA amplitudes we include the amplitudes for multiple scattering, allowing both the projectile to scatter twice and the two nucleons of the deuteron to rescatter. This calculation is an extension of Wallace's work<sup>9</sup> and is described in Ref. 1. We will refer to it as MS. Except for the kinematics, the calculation is nonrelativistic. The deuteron wave function is calculated from the Paris  $NN$  potential.<sup>12</sup> The half-off shell  $NN$  scattering amplitudes are replaced by on-shell amplitudes obtained from the VPI phase shifts of Arndt *et al.*<sup>13</sup> using the four momenta of the final state of the vertex being calculated. Although in principle at large recoil momenta the calculation becomes increasingly unreliable, the comparison with the data shown below indicates a surprising degree of agreement.

#### VI. EXPERIMENTAL RESULTS

The threefold differential cross sections  $d^3\sigma/d\Omega_3d\Omega_4dT_3$  along with the IA and MS calculations are presented in Figs. 1–6 as a function of  $T_3$ , where  $T_3$  is

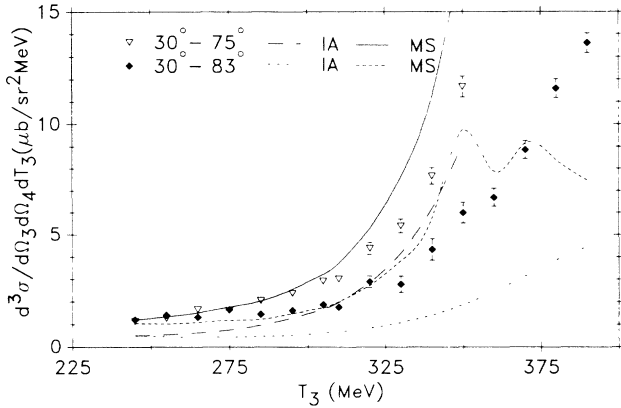


FIG. 1. Differential cross-section data for  $\theta_3=30^\circ$  and  $\theta_4=75^\circ$  and  $83^\circ$ . The curves are the IA and MS calculations. The MS calculations are the solid and short dashed lines and the IA calculations are the long dashed and dashed dotted line.

the kinetic energy of the proton observed in the MRS at an angle  $\theta_3$ . The other proton has a kinetic energy  $T_4$  and is observed at an angle  $\theta_4$ . The IA calculation includes the coherent addition of proton and neutron knockout amplitudes. From these figures it is difficult to see any clear relationships between the data and the calculations, except to note that in general the MS calculation comes closer to the data than does the IA. (We note that the calculations for the angle pairs at  $30^\circ-90^\circ$  and  $30^\circ-83^\circ$ , see Figs. 1 and 2, show structure that is not reproduced by the data.) The data cover a range of  $p_5$  from 200 to 674 MeV/c and one cannot sensibly express the data in terms of  $|\Phi(\mathbf{p}_5)|^2$  since, as described above, in the IA for this range of  $p_5$  both proton and neutron knockout are important, and in the case of neutron knockout,  $p_5$  no longer is equal in magnitude to the momentum of the struck nucleon in the initial state. Therefore in order to compare all the data to either the IA or MS calculations, in the subsequent figures we will show the ratio of the measured cross sections to either the IA or MS calculations as a function of various kinematic variables. The data will be divided into three parts. Those data for which  $\theta_3$  remained fixed at  $30^\circ$  will be re-

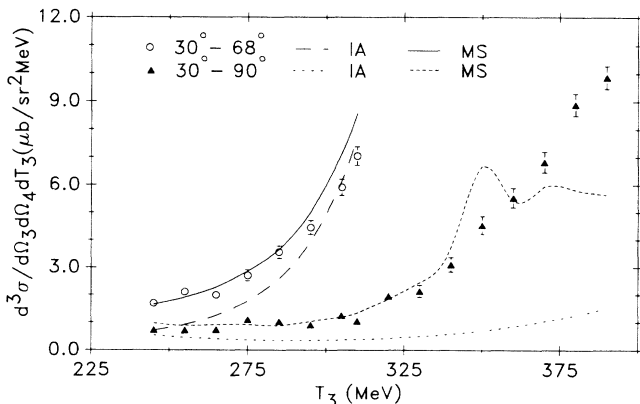


FIG. 2. Same as Fig. 1 for  $\theta_4=68^\circ$  and  $\theta_4=90^\circ$ .

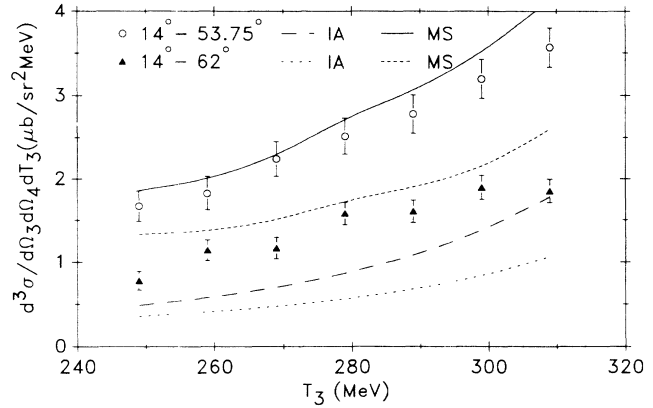


FIG. 3. Differential cross-section data for  $\theta_3=14^\circ$  and  $\theta_4=53.75^\circ$  and  $62^\circ$ . The curves are the same as in Fig. 1.

ferred to as the  $30^\circ$  data and those for which  $\theta_3$  was kept at  $14^\circ$  will be referred to as the  $14^\circ$  data. The remaining data will be referred to as set 3. The data divided by the IA and the MS as a function of  $p_5$  are shown in Figs. 7, 8, and 9. In these figures one sees that the IA does not agree well with the data, except for the lowest values of  $p_5$  for the  $30^\circ$  and set 3 data; i.e., the ratio of data/IA is almost always above 1.5. On the other hand the MS calculation agrees fairly well with most of the data over a range of  $p_5$  from 200 to about 530 MeV/c, although it has a tendency to overestimate the data for large  $p_5$ . In addition we note that even for data that disagree significantly with the MS calculation the ratio of data to MS varies from about 0.6 to 2, while for the IA the ratio of data to IA is often 6 or more.

In an attempt to gain at least a qualitative understanding of the nature of the comparison of the data with the calculations we will examine the ratio of the data to the MS calculation as a function of the relative kinetic energy of pairs of nucleons in the final state,  $T_{ij}$ . These ratios are shown in Figs. 10, 11, and 12. From these figures one sees that the data cover a range of  $T_{34}$  between 149 MeV to 318 MeV,  $T_{35}$  between 12 and 160 MeV, and  $T_{45}$  between 22 and 213 MeV. For low values of  $T_{ij}$  one antici-

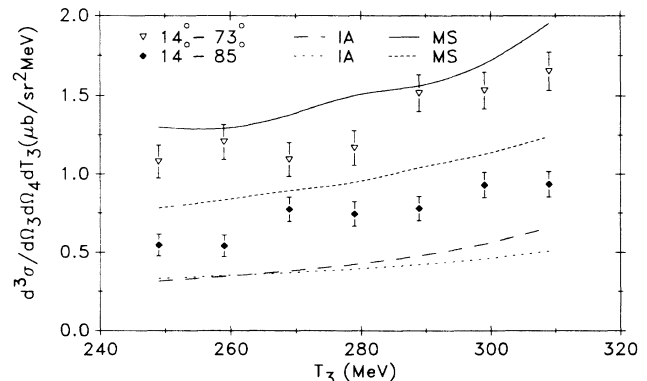


FIG. 4. Same as Fig. 3 for  $\theta_4=73^\circ$  and  $\theta_4=85^\circ$ .

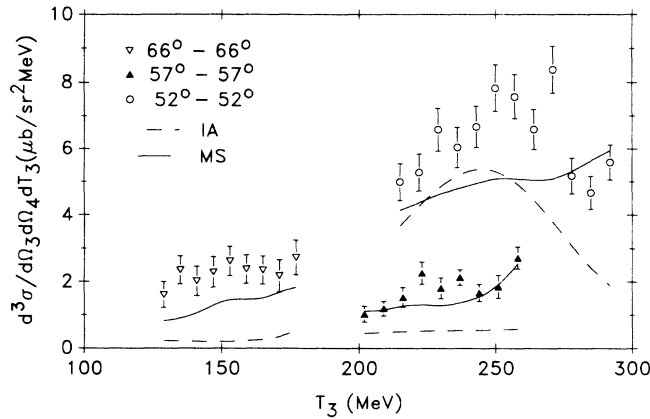


FIG. 5. Differential cross-section data for  $\theta_3=\theta_4=66^\circ$ ,  $57^\circ$ , and  $52^\circ$ . The MS calculations are the solid lines and the IA calculations are the long dashed lines.

pates that final-state interactions are an important component of the overall reaction mechanism, and for  $T_{ij}$  around 300 MeV one expects that virtual excitation of the  $\Delta$  resonance will be important. Obviously the real situation is more complicated since one must look at the coherent addition of all these processes. In Fig. 10 we show all the data divided by the MS as a function of  $T_{34}$ . For our data this is the only relative energy pair that covers the expected region of virtual  $\Delta$  excitation, and all our data except the  $14^\circ$  data are at or near  $T_{34}=300$  MeV. From Fig. 10 one sees that the ratio of data to MS is close to 1.0 except for two regions of  $T_{34}$ . One such region is around  $T_{34}=300$  MeV and, although it is difficult to see in the figure, almost all of the  $30^\circ$  data are between  $T_{34}$  of 275 to 318 MeV and some of these data are about a factor of 2 above the MS calculation. The second region where the data significantly exceed the MS calculation is a narrow peak around  $T_{34}$  of 250 MeV. The data in this second region were all taken at  $\theta_3=\theta_4=66^\circ$ . For these data  $p_4$  and  $p_5$  are both large and the IA contribution is essentially at a minimum. Recently Yano<sup>14</sup> has calculat-

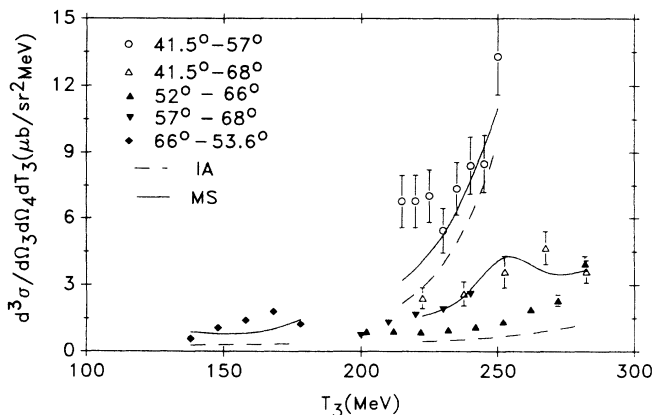


FIG. 6. Differential cross-section data for the following  $\theta_3-\theta_4$  angle pairs:  $41.5^\circ-57^\circ$ ,  $41.5^\circ-68^\circ$ ,  $52^\circ-66^\circ$ ,  $57^\circ-68^\circ$ , and  $66^\circ-53.6^\circ$ . The solid lines are the MS calculations and the long dashed lines are the IA calculations. Calculations are *not* presented for the  $57^\circ-68^\circ$  and  $52^\circ-66^\circ$  data.

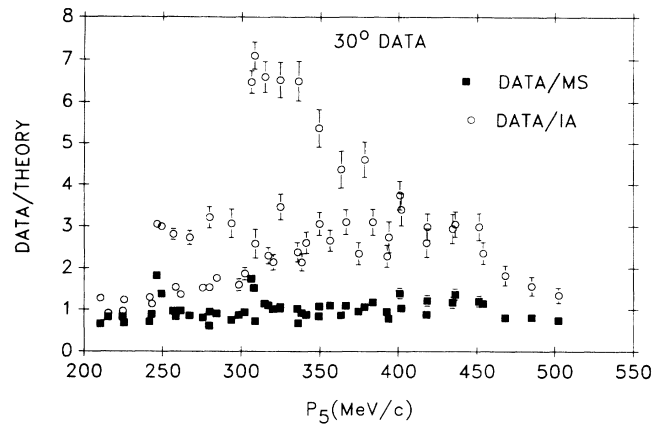


FIG. 7. The  $30^\circ$  data divided by the MS and IA calculations as a function of  $p_5$ .

ed the contribution of virtual  $\Delta$  excitation for these data using a Feynman diagram approach. His calculations show that virtual  $\Delta$  excitation is relatively strong here even though  $T_{34}=250$  MeV. This is due to the behavior of the pion propagator as well as to the peaking of the  $\Delta$  resonance near  $T_{ij}=300$  MeV. In Fig. 11 we show the data divided by MS as a function of  $T_{35}$ . In Fig. 12 all the data divided by MS vs  $T_{45}$  are shown. No clear pattern is evident in these figures. The apparent increase of the ratio of the  $30^\circ$  data to MS as  $T_{45}$  decreases is probably due to the fact that for these data  $T_{34}$  is also close to 300 MeV.

It appears that the MS calculation described above agrees well with the data if one excludes regions where one expects to see the effect of the  $\Delta$  resonance. This point is emphasized in Fig. 8 which shows only the  $14^\circ$  data divided by either the MS or the IA vs  $p_5$ . The  $14^\circ$  data are in a region of  $T_{34}$  between 149 and 251 MeV,  $T_{35}$  between 37 and 159 MeV and  $T_{45}$  between 165 and 213 MeV and one expects to be in a kinematic region that is almost always far from the effects of the  $\Delta$  resonance. The agreement with the MS is quite good. We should also note that the data of Aleshin *et al.*,<sup>10</sup> for the highest values of  $p_5$ , are in a kinematic region where  $T_{ij}$  is at

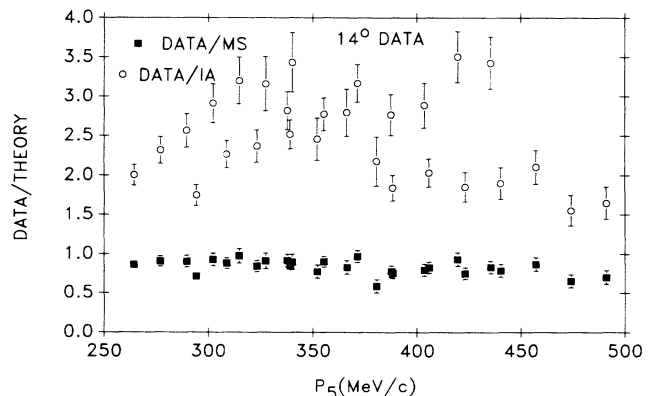


FIG. 8. Same as Fig. 7 for the  $14^\circ$  data.

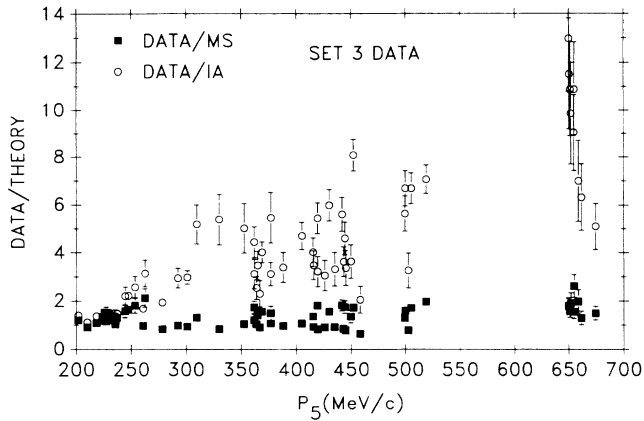
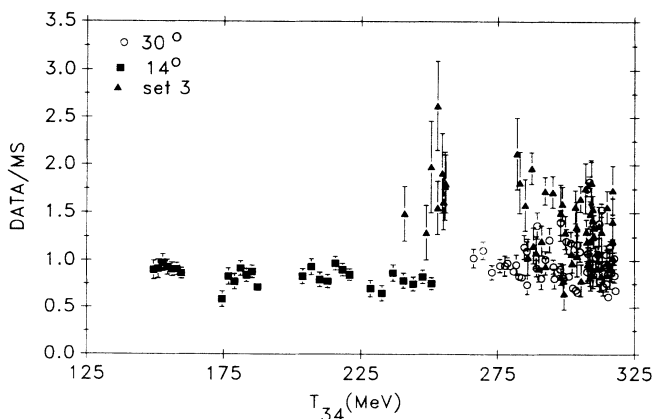
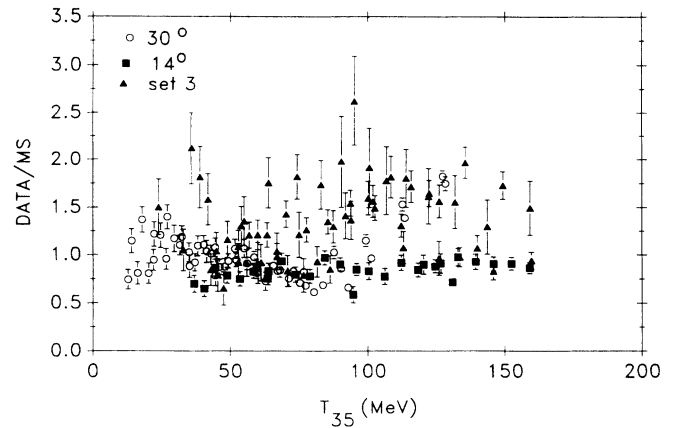


FIG. 9. Same as Fig. 7 for the set 3 data.

least 50 MeV away from the  $\Delta$  resonance. Their data at  $p_5$  near 150 MeV/c have  $T_{35} = 300$  MeV but are probably dominated by the IA terms and not noticeably affected by the  $\Delta$  resonance. Thus one might expect the good agreement between the data and the multiple scattering computation that is shown in their paper.

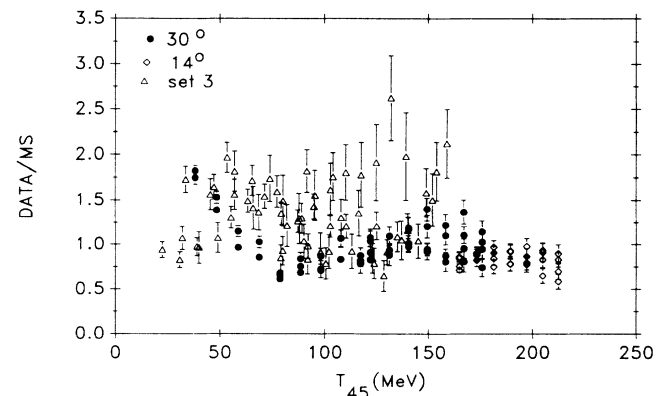
We stress that our discussion of the effects of the  $\Delta$  resonance in the  ${}^2\text{H}(p,2p)$  data presented here is at best only qualitative. For example, we note that in Fig. 10 there are data around  $T_{34} = 300$  MeV which agree quite well with the MS. One sees that the agreement with the MS calculation is quite good for some of the data points and somewhat poorer for the rest even though almost all of these data are in kinematic regions where we expect the  $\Delta$  resonance to be a strong influence. Clearly one needs better computations to understand these data. In particular one needs to calculate the amplitude for excitation of intermediate  $\Delta$  resonances as was done in Ref. 13 and coherently add this to the MS amplitudes. It is quite possible that the different ratios of the data to MS near  $T_{34} = 300$  MeV are due to constructive and destructive interferences between the  $\Delta$  amplitudes and the MS amplitudes. Moreover the MS part of the computation

FIG. 10. All the data divided by the MS calculation as a function of  $T_{34}$ . (Some of the  $30^\circ$  and set 3 data overlap around  $T_{34} = 300$  MeV.)FIG. 11. All of the data divided by the MS calculation as a function of  $T_{35}$ .

should be improved to include relativistic and off-shell effects. Nonetheless the MS computation shown here seems to be going a long way in successfully describing the data even in the  $\Delta$  region.

## VII. CONCLUSION

We have presented an accurate self-consistent set of  ${}^2\text{H}(p,2p)n$  data for  $200 < p_5 < 670$  MeV/c. The comparison of the data to the MS calculation suggests that one should be able to understand these results in terms of a calculation that includes multiple scattering and the excitation of intermediate  $\Delta$  resonances. Since some of the dynamics of  ${}^2\text{H}(p,2p)$  and  ${}^2\text{H}(e,e'p)$  reactions are very similar, such as multiple scattering between nucleon pairs in the final state, and, of course, the nuclear wave function is the same for both reactions, it may now be possible to use the data presented here to provide important constraints on the analysis of the  ${}^2\text{H}(e,e'p)$  data and thus provide a self-consistent way to use the  $(p,2p)$  and the  $(e,e'p)$  data to extract meaningful information about the high momentum components of the deuteron wave function. We also note that since these data span a significant portion of the width of the free  $\Delta$  resonance one might be

FIG. 12. All of the data divided by the MS calculation as a function of  $T_{45}$ .

able to use these data to study  $\Delta$ -nucleon interactions. We hope that our results will lead to the more detailed and accurate calculations that are clearly needed here.

#### ACKNOWLEDGMENTS

The success of this experiment would not have been possible without the important contributions made by the TRIUMF staff, in particular, D. A. Hutcheon, C. A. Miller, P. W. Green, and J. Tinsley. We also acknowl-

edge the help with the MS calculations provided by Jon M. Wallace at LANL, and phase-shift analysis provided by R. A. Arndt at Virginia Polytechnic Institute and Syracuse University. This work was supported by Grants PHY82-03431, PHY83-04320, PHY85-09880, PHY-8602662, PHYS-8905582, and PHY82-18386 from the National Science Foundation of the United States and by the Natural Sciences and Engineering Research Council of Canada. One of us (H.P.) is grateful for a NATO travel grant.

<sup>\*</sup>Present address: Istituto di Fisica, Universita di Milano, I-20133, Milano, Italy.

<sup>†</sup>Mailing address: TRIUMF, Vancouver, British Columbia, Canada V6T 2A3.

<sup>‡</sup>Present address: Pharma Department, Sandoz AG, CH4002 Basel, Switzerland.

<sup>§</sup>Present address: Jet Propulsion Laboratory, Pasadena, CA 91109.

<sup>\*\*</sup>Present address: University of Victoria, Victoria, British Columbia, Canada V8W 2Y2.

<sup>††</sup>Present address: Norfolk State University, Norfolk, VA 23504.

<sup>‡‡</sup>Present address: CAWCS, P. O. Box 10000, 1780 CA Den Helder, The Netherlands.

<sup>1</sup>V. Punjabi, K. A. Aniol, A. Bracco, C. A. Davis, M. B. Epstein, H. P. Gubler, J. P. Huber, W. P. Lee, D. J. Margaziotis, C. F. Perdrisat, P. R. Poffenberger, H. Postma, H. J. Sebel, A. W. Stetz, and W. T. H. van Oers, *Phys. Rev. C* **38**, 2728 (1988); V. Punjabi, C. F. Perdrisat, W. T. H. van Oers, P. R. Poffenberger, W. P. Lee, C. A. Davis, A. Bracco, D. J. Margaziotis, J. P. Huber, M. B. Epstein, H. Postma, H. J. Sebel, and A. W. Stetz, *Phys. Lett. B* **179**, 207 (1986).

<sup>2</sup>C. F. Perdrisat, V. Punjabi, M. B. Epstein, D. J. Margaziotis, A. Bracco, H. P. Gubler, W. P. Lee, P. R. Poffenberger, W. T. H. van Oers, Y. P. Zang, H. Postma, H. J. Sebel, and A. W. Stetz, *Phys. Lett.* **156B**, 38 (1985).

<sup>3</sup>S. Frullani and J. Mougey, in *Advances in Nuclear Physics*, edited by J. W. Negele and E. Vogt (Plenum, New York, 1984), Vol. 14, p. 1.

<sup>4</sup>P. Kitching, W. J. McDonald, Th. A. J. Maris, and C. A. Z. Vasconcellos, in *Advances in Nuclear Physics*, edited by J. W. Negele and E. Vogt (Plenum, New York, 1985), Vol. 15, p. 43.

<sup>5</sup>M. Bernheim, A. Bussière, J. Mougey, D. Royer, D. Tarnowski, S. Turck-Chieze, S. Frullani, G. P. Capitani, E. De Sanctis, and J. Jans, *Nucl. Phys.* **A365**, 349 (1981); S. Turck-Chieze, P. Barreau, M. Bernheim, P. Bradu, Z. E. Meziani, J.

Morgenstern, A. Bussière, G. P. Capitani, E. De Sanctis, S. Frullani, F. Garibaldi, and J. Mougey, *Phys. Lett.* **142B**, 145 (1984).

<sup>6</sup>H. Breuker, V. Burkert, E. Ehses, U. Hartfiel, G. Knop, G. Kroesen, J. Langen, M. Leenen, W. Mehnert, A. Samel, R. Sauerwein, H. D. Schablitzky, and G. Schnicke, *Nucl. Phys.* **A455**, 641 (1986).

<sup>7</sup>H. Arenhövel, *Nucl. Phys.* **A384**, 287 (1982).

<sup>8</sup>C. F. Perdrisat, L. W. Swenson, P. C. Gugelot, E. T. Boschitz, W. K. Roberts, J. S. Vincent, and J. R. Priest, *Phys. Rev.* **187**, 1201 (1969); T. R. Witten, M. Furić, G. S. Mutchler, C. R. Fletcher, N. D. Gabitzsch, G. C. Phillips, J. Hudomalj, L. Y. Lee, B. W. Mayes, J. C. Allred, and C. Goodman, *Nucl. Phys.* **A254**, 269 (1975); R. D. Felder, T. R. Witten, T. M. Williams, M. Furić, G. S. Mutchler, N. D. Gabitzsch, J. Hudomalj-Gabitzsch, J. M. Clement, G. C. Phillips, E. V. Hungerford, L. Y. Lee, M. Warneke, B. W. Mayes, and J. C. Allred, *ibid.* **A264**, 397 (1976).

<sup>9</sup>J. M. Wallace, *Phys. Rev. C* **5**, 609 (1972).

<sup>10</sup>N. P. Aleshin, S. L. Belostotsky, Yu. V. Dotsenko, J. Ero, O. G. Grebenynk, J. Kechkemeti, L. M. Kochenda, Zh. Kovach, L. G. Kudin, N. P. Kuropatkin, S. I. Manayenkov, O. V. Mikluho, V. N. Nikulin, O. E. Prokofjev, A. Yu. Tsaragorodtsev, and S. S. Volkov, Academy of Sciences, USSR, Gatchina, Report No. 1259, 1987 (unpublished).

<sup>11</sup>A. Bracco, H. P. Gubler, D. K. Hasell, W. T. H. van Oers, R. Abegg, C. A. Miller, M. B. Epstein, D. A. Krause, D. J. Margaziotis, and A. W. Stetz, *Nucl. Instr. Methods* **219**, 329 (1984).

<sup>12</sup>M. Lacombe, B. Loiseau, R. Vinh Mau, J. Coté, P. Pirés, and R. de Tournreil, *Phys. Lett.* **101B**, 139 (1981).

<sup>13</sup>R. A. Arndt, L. D. Roper, R. A. Bryan, R. B. Clark, B. J. VerWest, and P. Signell, *Phys. Rev. D* **28**, 97 (1983). Phase shifts from SAID, solution SP88 0-1.3 GeV.

<sup>14</sup>A. F. Yano, *Phys. Lett.* **156B**, 33 (1985).